Progress in Retinal and Eye Research xxx (2010) 1–10

Contents lists available at ScienceDirect

Progress in Retinal and Eye Research

journal homepage: www.elsevier.com/locate/prer

Intravitreal therapy for neovascular age-related macular degeneration and inter-individual variations in vitreous pharmacokinetics

Augustinus Laude [a,b], Lay Ean Tan [c], Clive G. Wilson [c], Gerassimos Lascaratos [a], Mohammed Elashry [a], Tariq Aslam [d], Niall Patton [e], Baljean Dhillon [a,*]

[a] Princess Alexandra Eye Pavilion, NHS Lothian, United Kingdom
[b] National Healthcare Group Eye Institute, Tan Tock Seng Hospital, Singapore
[c] Strathclyde Institute of Pharmacy & Biomedical Sciences, University of Strathclyde, United Kingdom
[d] Moorfields Eye Hospital, NHS Foundation Trust, United Kingdom
[e] Manchester Royal Eye Hospital, Central Manchester and Manchester Children's University Hospitals NHS Trust, United Kingdom

Keywords:
Intravitreal therapy
Age-related macular degeneration
Choroidal neovascularization
Pharmacokinetics
Vitreous
Injection

A B S T R A C T

This article aims to provide an interpretation and perspective on current concepts and recent literature regarding the evidence for individualizing intravitreal therapy (IVT), particularly considering iatrogenic and patient factors in the management of neovascular age-related macular degeneration (AMD). As ocular parameters that govern IVT pharmacokinetics do vary between individuals with AMD, developing a personalized strategy could improve safety and efficacy. This has to be derived from clinical measurements and data from laboratory animals; however, it is recognized that the animal models used in the development of intraocular formulations differ in their vitreous geometry from humans. These factors may be of relevance to the design of ophthalmic formulations and optimizing treatment outcomes in AMD. Further studies are needed to drive improvements in clinical practice which are aimed at maximizing the efficacy profile in IVT for AMD by a more rigorous evaluation of patient and surgeon-related variables.

Contents

* Corresponding author. Department of Ophthalmology, Princess Alexandra Eye Pavilion, Chalmers Street, Edinburgh EH3 9HA, United Kingdom. Tel.: +44 (0) 131 5363901; fax: +44 (0) 131 5363897.
E-mail address: bal.dhillon@luht.scot.nhs.uk (B. Dhillon).

1350-9462/$ – see front matter © 2010 Elsevier Ltd. All rights reserved.
doi:10.1016/j.preteyeres.2010.04.003

1. Introduction

Intravitreal therapy (IVT) employing anti-vascular endothelial growth factors (anti-VEGF) represents a paradigm shift in the management of neovascular age-related macular degeneration (AMD). IVT has been supported by promising results in clinical trials and is now endorsed as a strategy to target submacular choroidal neovascularization in patients with AMD. In translating trial data to clinical practice, it is hoped that patients may experience improvement in best-corrected visual acuity. This was hitherto not achievable by previous treatment modalities, including thermal laser photocoagulation and photodynamic therapy (PDT).

Approval of ranibizumab by some United Kingdom National Health Service funding agencies has led to a rapid increase in the use of IVT in the treatment of AMD. The standardization of drug dosage, injection volume and technique has been recommended, based on clinical trial data and the adoption of recommendations from the Royal College of Ophthalmologists and National Institute of Clinical Excellence. These data however do not account for the potential sources of variation in the pharmacokinetics and efficacy influenced by ocular anatomy and IVT techniques. Furthermore, previous reports found that a proportion of patients with AMD treated by repeated IVT failed to respond or showed progressive loss of vision. Identifying predictive factors for anti-VEGF treatment response thus remain a priority for individualizing IVT in AMD.

The literature was reviewed by interpreting selected data relating to recent IVT-related publications in order to determine the potential therapeutic impact of anatomical characteristics, including biometry, vitreous state and intraocular pressure, previous intraocular surgery and phakic or pseudophakic status. In addition, we searched for published data on the impact of needle bore, scleral injection site placement, formulation effects on the deposition and clearance of the injected drug.

2. Anatomical and biochemical factors

2.1. Elimination pathways and barriers to drug absorption

The late David Maurice elegantly demonstrated, using fluorimetry, the two major routes of elimination for molecular probes from the vitreous (Maurice, 1976). The vitreous is surrounded by the retina and thus the most direct pathway out is through this tissue. If this route is unavailable, it was argued that material travels forward to be eliminated via the anterior route through the aqueous humour. Barza and colleagues' work supported this hypothesis (Barza et al., 1982), whereby in the presence of systemic probenecid, the measured half-life of intravitreally administered carbenicillin was increased from 5 to 13 h in the rabbit and the aqueous humour concentrations increased by approximately ten-fold. This dramatic demonstration revealed an active transport process in the retina that aided the removal of drug from the vitreous.

The established barriers to drug absorption in the eye are the inner blood-retinal barrier (BRB) provided by the endothelium of the retinal capillaries near to the vitreous surface and the outer BRB provided by the retinal pigment epithelium (RPE). The first layer abutting the vitreous is the inner limiting membrane (ILM) of the retina. Originally thought to be an extension of the Muller cells, the ILM appears to be formed from both neural and vitreous components (Heegaard et al., 1986). It has been suggested that the ILM could form a diffusion barrier, particularly for large charged cationic species (Pitkanen et al., 2004), although it is possible that the binding of the delivery construct to collagen within the vitreal cortex itself limits exposure (Peeters et al., 2005). Histological studies of the retinal penetration of bevacizumab in monkeys using Cy-3-conjugated IgG antibody showed rapid movement to the RPE within 4 days, although the ILM was noted to be stained up to 14 days post-injection, suggesting some modulation effect by the membrane (Heiduschka et al., 2007).

2.1.1. Effects of vitreous volume and vitreous diffusional path length

The vitreous humour fills the region between the lens and the retina where it is attached anteriorly to the ora serrata, ciliary epithelium, zonular fibres and posteriorly to all of the retina unless there is a posterior vitreous detachment (PVD). It occupies 80% of the eye globe and has a volume and wet weight of approximately 4 mL and 4 g respectively. The main component of the vitreous humour is water (~98–99% w/w), with a microstructure of collagen and glycosaminoglycans (hyaluronan, chondroitin sulphate and heparan sulphate) conferring viscoelastic properties. The vitreous diffusional path length measures the distance from the injection site to the macula.

In the simplest calculation, starting by ignoring convective flow and local variations in viscosity, an agent such as a drug for the treatment of AMD injected as a solution into the vitreous compartment will diffuse through the gel driven by the concentration gradient. This is especially true for small molecules, where forces of diffusion predominate. Whilst the VEGF binding may be specific within the retina, the bulk drug movement towards the posterior pole would be expected to approximate to a function of gel dimensions. Vitreous volume may be calculated by assuming the globe volume approaches a πr^3 spherical geometry, minus the lens ellipsoid. Concentrations in the vitreous can be used to calculate the exposure to the retina and macula, assuming equilibrium conditions apply. Changes in vitreous viscosity, composition and vitreous gel movement (with eye position) may be modeled to assess their impact on drug distribution.

2.1.2. Models and their shortcomings

There are no published validated techniques for human vitreous volume estimation in vivo. However, volume could be estimated using anatomical similarity to mathematical geometric forms. This has been applied elsewhere: for example, techniques of approximation to the ellipsoid geometric form have been used in ultrasound measurements of tumour volume of choroidal melanomas (Richtig et al., 2004). An ellipsoid is a geometric surface, all of whose plane sections are either ellipses or circles. In assessing total volume of vitreous cavity, one could assume vitreous to be a partial ellipsoid minus a smaller partial ellipsoid (the lens) (Restori, personal communication), and the volume of these ellipsoids can be calculated using the equation;

$$V = 4/3\pi abc$$

where V is vitreous volume; a and b are the equatorial radii (along the x and y axes) and c is the polar radius (along the z-axis). Estimation of

Please cite this article in press as: Laude, A., et al., Intravitreal therapy for neovascular age-related macular degeneration and..., Progress in Retinal and Eye Research (2010), doi:10.1016/j.preteyeres.2010.04.003

vitreous volume can then be deduced using B-scan (or A-Scan) to measure the vitreous length and B-Scan to measure the vitreous diameter and the lens radii (Restori, personal communication).

Similarly one could assume the vitreous as a partial sphere and use the formula for a partial sphere (LMNO Engineering) to estimate vitreous volume (V):

$$V = (\pi/3)y^2(1.5D - y)$$

where V is the vitreous volume; y is the distance from posterior pole to vitreous base and D is the axial length of the eye.

These techniques are likely to include errors from necessary simplification of the eye anatomy when compared to the perfect geometric models. An alternative way would be to establish, using ultrasound B-scan, the volume of a body by making serial parallel scans at fixed intervals and measuring the cross sectional area of the body on each scan (Lunt, 1978). The results may be combined to give the volume by summing the areas and multiplying by the interval between the scans. All sections must of course be at the same angle in the body. This technique can be applied to ophthalmic use for calculation of vitreous volume. Although more time consuming, this avoids the errors from techniques involving approximation of the vitreous as sections of perfect geometric forms.

Laboratory animals including mice and rabbits are frequently used as models in pharmacokinetic studies. Nevertheless, interspecies anatomical differences, especially vitreous volume and vitreous diffusional path length, may make the direct allometric translations of data to the human model unreliable. The vitreous volume in the rabbit is around 1.5 mL, about one third the vitreous volume in man. In a direct comparison, in terms of initial concentration, the amount achieved in the human eyes would only be about 35% of that in the rabbit. This discrepancy in vitreous volumes could account for the differences in the estimated pharmacokinetic parameters since a larger vitreous volume would imply a longer duration required for equivalent distribution.

In addition, a difference in vitreous diffusional path length affects drug distribution. Hughes and colleagues collated the results from histological examinations which were in part previously reported by Short in 2008 as shown in Fig. 1 (Hughes, 2008; Short, 2008). From these cross-sections, the authors calculated the theoretical diffusional distances across the eye and the data illustrates the dramatic differences. For example, the vitreous diffusional path length in the rat and rabbit is estimated to be 4.4 mm and 9 mm respectively compared to the distance in the human of 22 mm. Since the diffusional drive decreases according to the square root of time, the resulting concentrations at a distant target risk being too small to be effective from a depot placed in the anterior globe. In terms of clearance, the shorter vitreous diffusional path length in rabbits decreases the half-life by 1.7 times for posterior clearance and is twice as fast for anterior clearance as compared to humans (Maurice and Mishima, 1984). In a recent study by Zhu et al. (Maurice, 2001; Zhu et al., 2008), the terminal half-life of bevacizumab in humans was shown to be 6.7 days compared to 4.3 days measured in the rabbit (Bakri et al., 2007).

Assuming a molecule diffuses through a static continuous phase, all effects relate to the concentration gradient and the ability of Brownian motion to equilibrate the molecule through parts of the gel. On the other hand, if deposition or clearance occurs at the boundary of the envelope, or flow processes exist that are largely uni-directional, a concentration gradient may be generated. The engineering description of this is embodied in the Peclet number, which allows the relative contribution of diffusion and convection to overall drug distribution to be attributed (Park et al., 2005; Stay et al., 2003; Xu et al., 2000). As has been mentioned, small

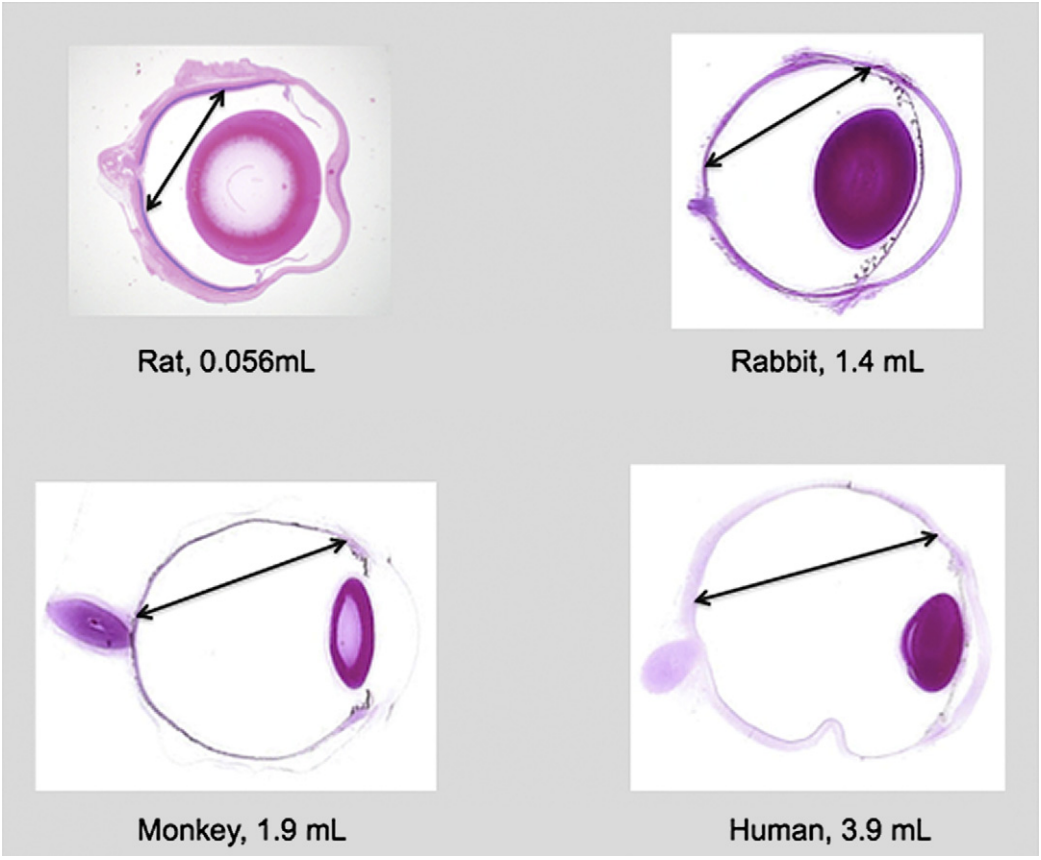

Fig. 1. Examinations of the histological cross-sections of animal ocular tissues (Hughes, 2008).

Please cite this article in press as: Laude, A., et al., Intravitreal therapy for neovascular age-related macular degeneration and..., Progress in Retinal and Eye Research (2010), doi:10.1016/j.preteyeres.2010.04.003

laboratory animals especially mice and rabbits have a shorter vitreous chamber as compared to man (Table 1) and a shorter vitreous diffusional path length. These factors underestimate the contribution of convective flow (Stay et al., 2003; Xu et al., 2000). This process will be important in the elderly, synchitic eye where convective flow is enhanced by the local pool of liquid vitreous formed during the ageing process. Thus, the combination of geometric difference and liquefaction has the consequence that data obtained in the studies on small animals is not likely to reflect the actual clinical outcomes expected in elderly human subjects.

The anatomical characteristics of the elimination pathway may also affect intravitreal half-life as the diffusional path through the vitreous to the retina is shorter than that to the anterior chamber. The mean transit time for tritiated water to traverse the distance from the mid-vitreous to the choroid in the anesthesized rabbit is 32 min versus 84 min for anterior chamber to the choroid (Moseley et al., 1984). The authors considered these differences to be entirely explained by diffusion and that bulk flow was unimportant. The rate of drug clearance is inversely proportional to the vitreous diffusional path length, which predicts a higher clearance in smaller animals. In addition, the larger retinal surface and capacity for active transport may increase posterior clearance. Overall, the divergence of clearance rates from anterior and posterior elimination pathways increases with molecular weight (Maurice, 2001). These factors, as well as convective flow patterns, could apply to intravitreal delivery of anti-VEGF agents.

2.1.3. *Vitreous humour as a barrier to diffusion*

Although the solid content of the vitreous humour is relatively small (~1%), the alignment of collagen and glycosaminoglycans as shown in Fig. 2 is sufficient to maintain the rigidity and stability of the gel and more critically, acts as a molecular barrier to diffusion. Accordingly, the diffusion of materials through the vitreous would be expected to deviate sharply from that in water. If the eye is treated with hyaluronidase, the movement of materials from mid-vitreous to choroid is significantly faster (exponential half-life 36 ± 13 min in controls compared to 20 ± 7 min in treated animals) suggesting that structural elements constituted by the vitreous components do contribute to the overall rate of material transport (Foulds et al., 1985). Small molecules with low molecular weight (MW) encounter lower steric hindrance and hence their migration in the vitreous is largely diffusive (Park et al., 2005). Injection via the pars plana into the anterior segment of the vitreous chamber allows free diffusion in all directions towards the anterior chamber and retina (Lund-Anderson and Sander, 2003). The intravitreal half-life of low MW substances is usually a few hours but as the MW rises above 10,000 daltons, clearance slows. For instance, the intravitreal half-life of dexamethasone (MW = 392 Da) is 5.5 h in humans, as compared to 25 h for vancomycin (MW = 1.5 kDa).

Table 1
Comparative weight and volume of the vitreous humour in different species.

Species	Weight of vitreous humour (g)	Volume of vitreous humour (mL)	Length of vitreous path length (cm)	Aqueous flow (μL/min)
Human	3.9[a]	3.9–5.0[d]	1.65[b]	2.5–3.0[d]
Sheep	8.1[a]	8.0[a]	2.10	
Pig	3.6[a]	3.5[a]	1.70	
Mouse			0.08	
Rabbit	1.4–1.7[d]	1[a]	0.78[c]	3.6[d]
Ox	15.0[a]	16[a]		

[a] Jaffe (1969).
[b] Lund-Anderson and Sander (2003).
[c] Park et al. (2005).
[d] Meredith (2006).

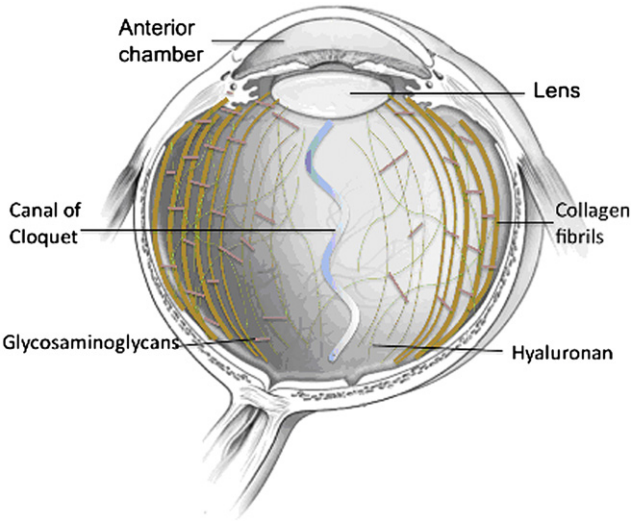

Fig. 2. Microstructure of the vitreous humour.

Table 2 illustrates more examples of the difference in terminal half-life of compounds of different MW. The movement of larger molecules is also dependent on the intravitreal outflow (convection), which is generated by pressure and temperature differences between the anterior chamber and the surface of the retina. Head and eye movements may also contribute although the hydraulic effects are probably unimportant (Missel, 2002), except perhaps during injection when excess pressure is generated by expansion of the vitreous volume and temporary destruction of vitreous integrity. The effect of convection has been simulated and is proposed to account for approximately 30% of the intravitreal transport of small molecules. For larger molecules, when the diffusion process is limited, it becomes the main transport mechanism (Xu et al., 2000).

2.2. *Changes in the vitreous composition and consequences of synchisis and posterior vitreous detachment*

With ageing in the fifth and sixth decades, the vitreous humour undergoes progressive syneresis and synchisis resulting from the aggregation of collagen fibres and segregation of hyaluronan. Consequently, thickened and tortuous collagen fibres and cavity formation in the liquid vitreous gradually become apparent, ultimately followed by the collapse of the gel-phase. By the eighth and ninth decades, almost half of the gel-phase has turned into a liquid phase. Hence, in comparison with a juvenile vitreous humour, areas within an ageing vitreous that undergo liquefaction and contraction are less elastic and less viscous with a high content of non-gel associated water. This will have a significant impact on drug distribution and elimination, since the nature of the diffusional

Table 2
Intravitreal half-life comparison of small and large molecular weight drug compounds.

Compound	MW	Terminal half-life	Study model	References
Ganciclovir	255 Da	7.1 h	Rabbit	(Lopez-Cortes et al., 2001)
Dexamethasone	392 Da	5.5 h	Human	(Gan et al., 2005)
Gentamycin	464 Da	33 h	Monkey	(Barza et al., 1983)
Vancomycin	1.5 kDa	25 h	Human	(Aguilar et al., 1995)
Ranibizumab	48 kDa	3 days	Monkey	(Gaudreault et al., 2005)
Bevacizumab	149 kDa	4 days	Rabbit	(Bakri et al., 2007)

Please cite this article in press as: Laude, A., et al., Intravitreal therapy for neovascular age-related macular degeneration and..., Progress in Retinal and Eye Research (2010), doi:10.1016/j.preteyeres.2010.04.003

barrier has altered. These changes were illustrated by using vitreous fluorophotometry by our group (Tan, 2009). Fluorophotometric methods have been employed since the 1980s to assess the permeability of BRB in normal (Moldow et al., 1999; Oguro et al., 1985) and disease eye models including early age-related maculopathy (Moldow et al., 2001), diabetic macular edema (Sander et al., 2001) and retinitis pigmentosa (Moldow et al., 1998).

It is evident that degeneration of the vitreous humour with age increases vitreous diffusivity and diminishes the formation of drug concentration gradient across the medium. Tan and coworkers established the first study that quantitatively analysed the impact of vitreous liquefaction on material movements in a partially liquefied rabbit vitreous model generated using hyaluronidase. In this study, both small and large molecules were distributed and cleared faster in the liquefied vitreous model as compared to normal vitreous (Tan, 2009). In addition, the diffusion coefficients of fluorescein recorded from subjects with retinitis pigmentosa were reported to be higher (8.0×10^{-6}–2.3×10^{-5} cm/s^2) than in healthy subjects (3.9–7.5×10^{-6} cm/s^2) (Moldow et al., 1998). While it is possible that this could be related to less retina that is normally functioning, it could also indicate both a loss of vitreous barrier function and greater vitreous stirring caused by the convective flow in the more liquefied areas of the vitreous (Fishman et al., 1981; Prager et al., 1982). Furthermore, Maurice noted that the effects of vitreous liquefaction are more significant in the region where the concentration gradient is present and where the effects of enhanced convective flow are maximal (Maurice, 2001).

The incidence of PVD increases with age as a consequence of vitreous degeneration. The liquefied and contracted vitreous produces a tractional force that pulls the vitreous cortex away from the retina, generating two compartments within the chamber as shown in Fig. 3. The detachment of the vitreous at the back of the eye could also provide altered passage of material in the vitreous, since movements of the head will stir the remnants of the liquid phase of the detached vitreous. This pattern may be distinctive to a particular type of PVD where the detachment point occurs at the superior half of the posterior segment (Yoshida et al., 1984). In addition, the higher concentration of fluorescein observed clinically in the mid-vitreous of eyes with established PVD is thought to be caused by the greater influx of fluorescein from the subhyaloid space which is located in closer proximity to the mid-vitreous when it is detached (Moldow et al., 1998; Prager et al., 1982; Yoshida et al., 1984). Thus drug distribution and clearance within a PVD model will be different from that of a healthy vitreous owing to the imperfection of the vitreo-retinal adherence.

In addition, the accumulation of proteins in the remnants of the vitreous compartment should cause an unequal distribution of protein-bound drugs in terms of mass, though free concentration will be in equilibrium.

2.3. Effects of vitrectomy and vitreous substitutes

Depending on the clinical indications, the removal of vitreous through vitrectomy necessitates its replacement either by gas or fluid. Patients receiving anti-VEGF therapy have a small but significant risk (approximately 0.02%) of rhegmatogenous retinal detachment which could necessitate a vitreous substitute (Wu et al., 2008). The effect of vitreous substitutes (silicone oil, intravitreal gas or high density silicone oil) on the pharmacokinetics of anti-VEGF therapy has not been extensively investigated although any vitreous substitute could potentially represent a significant barrier to diffusion for IVT.

As the resistance to flow in the vitrectomized eye is reduced, the role of convective flow on drug movements becomes more important. For instance, the half-life of intravitreally injected triamcinolone acetonide was 2.9 days in non-vitrectomized rabbit eyes as compared to 1.6 days in vitrectomized eyes (Chin et al., 2005). In addition, vitrectomy has been associated with increasing drug clearance in aphakic eye models in kinetic studies of antibiotic deposition (Ficker et al., 1990; Meredith et al., 1995). Lee and colleagues have also shown faster VEGF clearance in vitrectomized as compared to non-vitrectomized rabbit eyes (Lee et al., 2010). According to findings by Knudsen and colleagues using fluorescein as a marker (Knudsen et al., 2001), this observation may be partly related to the alteration of the BRB caused by vitrectomy. It is also possible that vitrectomy may effect a change in diffusivity and drug solubility in the vitrectomized eye, as determined by the Stokes–Einstein equation which predicted that diffusion is inversely correlated with viscosity of the medium (Gisladottir et al., 2009). These data strongly suggest that clearance of intravitreally delivered drugs can be altered in a vitrectomized eye model.

Intravitreal gas bubbles resulting from injection of air, sulfur hexafluoride or perfluoropropane post-operatively could induce subclinical breakdown of the blood aqueous humour barrier (Ogura et al., 1989) which might result in the alteration of the pharmacokinetics of subsequent IVT.

Silicone oil is used for retinal tamponade as a vitreous substitute although usually for a limited period. If drug were to be administered in this vehicle, the release of drugs from silicone oil can be expected to follow either square root time kinetics if diffusion through the oil is rate limiting or first-order kinetics if partitioning

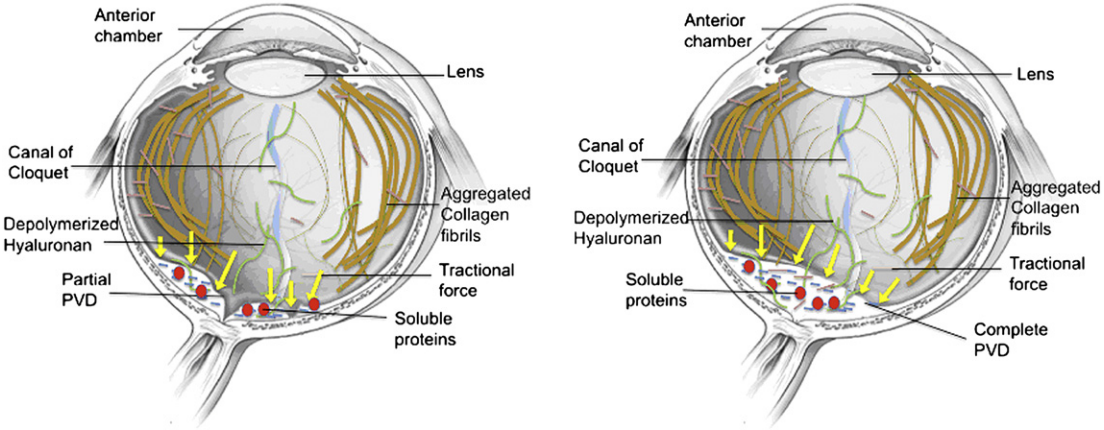

Fig. 3. Partial and complete PVD.

out of the oil into the vitreous is rate limiting (Jaffe, 1969). However, as work to date demonstrates little in the way of retinal toxicity to any of the three anti-VEGF drugs used (Foy et al., 2007; Fung et al., 2006; Rosenfeld et al., 2005), most clinicians to date have not reduced the dosage of anti-VEGF therapy, when injecting into silicone oil-filled eyes. For example, Falavarjani and colleagues (Falavarjani et al., 2010) injected 2.5 mg Avastin into five eyes with silicone oil tamponade for rubeotic glaucoma secondary to proliferative diabetic retinopathy and demonstrated no signs of toxicity, despite using double the normal dose, with potentially very high pre-retinal concentrations. Singh and Stewart reported on an individual with silicone oil tamponade in situ treated for iris neovascularisation with 1.25 mg bevacizumab, without any evident clinical toxicity (Singh and Stewart, 2008). On the other hand, silicone oil is also known to cause proteins to aggregate and so may potentially inactivate VEGF inhibitors.

However, whilst the insolubility of the anti-VEGF drugs within vitreous substitutes could lead to a corresponding reduction in the available space for the drug to disperse, and hence a much greater pre-retinal/intravitreal fluid concentration, the absence of evident clinical toxicity suggests that most clinicians do not consider the vehicle to be an issue when administering the drugs.

2.4. Effects of lens status

Since anti-VEGF drugs are transported from the vitreous cavity into the aqueous humour through the lens zonules between the lens and the ciliary body (Bakri et al., 2007; Gaudreault et al., 2005), patients that have had previous cataract surgery might have more rapid clearance of the drug from the eye, as has been shown experimentally with intravitreal triamcinolone (Schindler et al., 1982), amikacin (Mandell et al., 1993), gentamicin (Cobo and Forster, 1981) and vancomycin (Pflugfelder et al., 1987).

3. Drug related factors

3.1. The impact of transporters

With regards to controlled drug delivery systems, the issue of transporters is likely to be important as the release rate is likely to be slow and sustained and therefore the concentration gradient, which normally drives drug equilibration, may be modest. As a consequence, there has been a lot of interest in the expression of transporter types in ocular tissues (Hughes et al., 2005). Urti's group commented that the highest impact will be seen, in terms of pharmacokinetics, when passive diffusion is low and the transporter is on the rate limiting pathway (Mannermaa et al., 2006). As a corollary, saturation of an efflux pathway might not occur (Mannermaa et al., 2006). The application of transporter inhibition to increase drug exposure to the retina from the vitreal side has been pursued experimentally-for example, the L-Valine monoester pro-drugs of ganciclovir (val-GCV and val-val-GCV) are eliminated faster from the vitreous humour faster than the parent drug whereas gly-val-GCV was slower. However, retinal ganciclovir concentrations were almost identical at the end of 5 hours' exposure (Majumdar et al., 2006). The impact of transporters is thus suspected to be important but our knowledge of the contribution is limited and will require further investigation.

3.2. Drug distribution and finite element analysis

Two common methods encountered in the modelling of drug distribution are compartmental modelling and finite element analysis. Compartmental modelling is widely used by physiologists to describe systems which are linked; for example absorption from

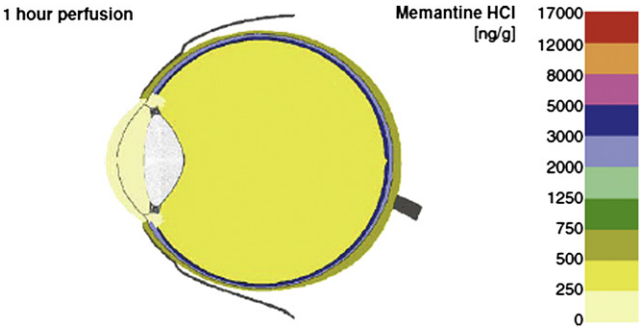

Fig. 4. Compartmental model of the intravitreal deposition of memantine in the rabbit eye (Koeberle et al., 2006).

an intravitreal injection can be thought of as events occurring in different 'boxes': the vitreous, the retina and the anterior chamber. The measurements are derived from small numbers of whole tissue samples and provide a simple description of changes in concentration with time. In contrast, finite element modelling allows the use of digital measurements such as magnetic resonance imaging (MRI) or scintigraphy (more sample spaces at each time) and the partial differential equations are solved by considering the areas of interest as a meshwork of prisms or other geometric shapes. This is much more descriptive but takes more computing power. However, both the compartmental and the finite element models use partial differential equations to approximate the behaviour in small increments (dt). Fig. 4 is taken from a study in which the putative neuroprotective agent memantine was applied by different routes to a perfused bovine eye. In this case, the distribution following direct injection into the vitreous is shown. Only a crude map of distribution is possible and local variations are not mapped.

In contrast, a finite element model typical breaks down the volume into prismatic voxels and the interaction of each voxel with surrounding voxels is calculated (Fig. 5). Specific ocular dimensions of the studied species, tissue compartments as well as boundary conditions surrounding the tissues can be defined within the model. In addition, general assumptions including the hyaloid membrane imposes no resistance to fluid flow for the anterior transport and highly vascularized choroidal circulation acting as

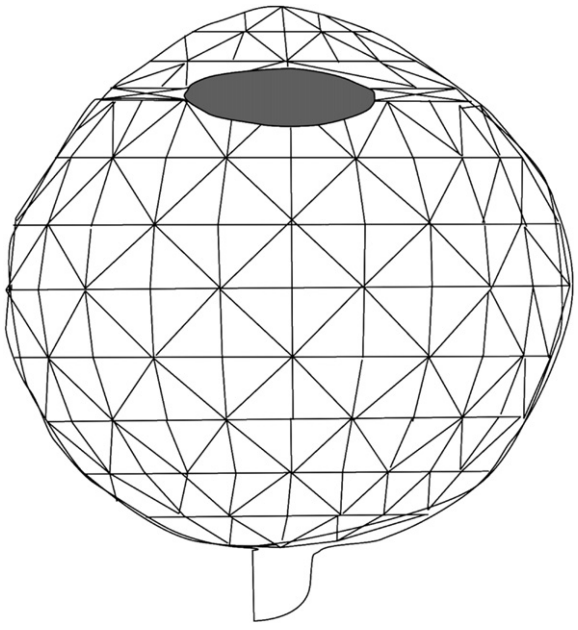

Fig. 5. Illustration of ocular meshwork used in finite element analysis.

Please cite this article in press as: Laude, A., et al., Intravitreal therapy for neovascular age-related macular degeneration and..., Progress in Retinal and Eye Research (2010), doi:10.1016/j.preteyeres.2010.04.003

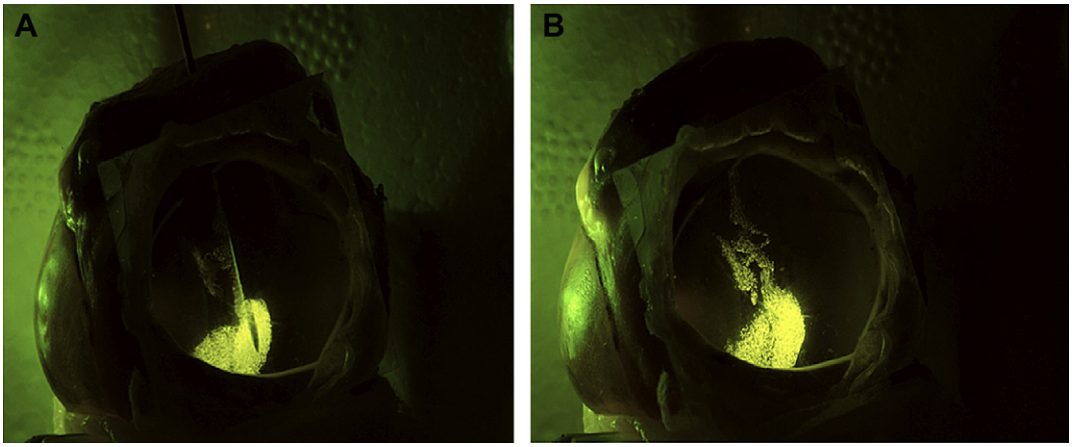

Fig. 6. Imaging of intravitreally injected 10 μm particles through the Miyake-Apple window. (A) During injection; (B) After injection.

a perfect sink for retinal drug clearance have been made to mimic physiological conditions. Incorporation of the studied parameters (such as the size and shape of injection, molecular size of drug molecules and vitreous diffusivity) into the designed model allows drug concentration profiles to be predicted locally. For example, the concentration–time profile of drugs administered following intravitreal injection and implant under different rates of aqueous and vitreous outflow have been simulated by Park et al. (2005) while Friedrich et al. (1997) predicted the pharmacokinetic profiles of fluorescein and fluorescein glucuronide at different positions within the vitreous chamber as a consequence of intravitreal injection position, volume and pathophysiological conditions.

It is often assumed that the shape of injection is a bleb occupying a volume that is approximately spherical or cylindrical. This assumption is frequently the starting point in finite element modelling; however, the true picture is best described as a wavy needle track leading to and beyond the injection pocket as shown in Fig. 6.

It should be appreciated that the injections of particulates compared to solutions produce very different initial distributions in the vitreous. For example, injection of particles outlines a pocket as shown in the Miyake-Apple preparation above and resembles the picture seen when the suspension is injected into vitreous humour in a cuvette (Fig. 7). The structures seen relate to the cisternal anatomy of the vitreous, first elegantly defined by the injection of Indian ink into various sections of dissected eyes (Jongebloed and Worst, 1987).

3.3. Drug formulation variables and dosing schedule

The relationship between dosing frequency and efficacy has been investigated previously. Differences in the pharmacokinetic profiles of different anti-VEGF agents were uncovered during the pre-clinical investigations. The animal studies showed that after residing in the vitreous humour for 28 days, pegaptanib sodium was still able to bind to $VEGF_{165}$ (Drolet et al., 2000). There was also sufficient concentration of the drug present in the vitreous after 28 days of a single intravitreal injection, well above the K_D for VEGF (200 pM) binding, which led to the suggested dosing frequency of

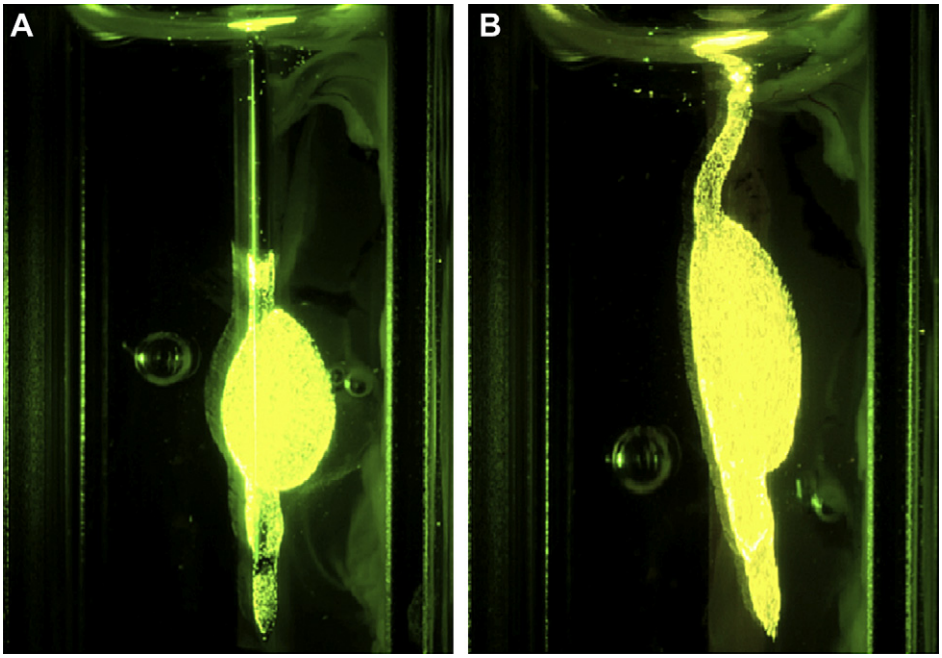

Fig. 7. Imaging of fluorescent 10 μm particles injected into a cuvette contained dissected and carefully decanted ovine vitreous. (A) During injection; (B) After injection. This pattern stays stable for at least 5 h, and particles settled without diffusing through the media.

Please cite this article in press as: Laude, A., et al., Intravitreal therapy for neovascular age-related macular degeneration and..., Progress in Retinal and Eye Research (2010), doi:10.1016/j.preteyeres.2010.04.003

every 6 weeks for pegaptanib sodium, compared to every 4 weeks for ranibizumab (Eyetech Study Group).

The current first line IVT is ranibizumab and the monthly dosing employed by the MARINA and ANCHOR studies, though associated with good efficacy, may be limited in practice by issues such as patient compliance and cost of treatment (Mitchell et al., 2010). The observation that most of the visual acuity improvement occurred within the first 3 months led to the widespread adoption of an initial loading dose of monthly injections repeated 3 times followed by different repeat injection frequencies. The PIER study used fixed 3 monthly repeated injections while the PRONTO study used a 1 monthly 'as needed' (PRN) protocol based on predetermined criteria (Mitchell et al., 2010) and it was observed that the PRONTO study achieved a better outcome compared to the PIER study, suggesting the importance of adequate dosing frequency in order to achieve and maintain the efficacy of this treatment modality.

Furthermore, a direct comparison of different treatment frequency regimes was performed in the recent EXCITE trial (Eter, 2008). This was a Phase IIIb multicenter, randomized, active-controlled, double-masked trial of all CNV types that compared monthly injections with receiving 3 monthly injections followed by quarterly injections. Interestingly, monthly injections of 0.3 mg ranibizumab ($n = 101$) were shown to result in a greater mean VA improvement from baseline at 12 months (+8.3 letters) compared with quarterly injections of either 0.3 mg ($n = 104$) or 0.5 mg ($n = 88$) ranibizumab (+4.9 and +3.8 letters, respectively). Thus, monthly injections appeared to have a better outcome compared to quarterly injections (Eter, 2008). In another retrospective, interventional case series involving 131 eyes with treatment-naïve, exudative AMD undergoing ranibizumab monotherapy, more frequent injections (on average 1 injection every 1–2 months) were associated with a greater mean VA improvement and a lower proportion of eyes with moderate vision loss than less frequent injections (Dadgostar et al., 2009). To date however, there is not sufficient evidence to consistently demonstrate outcomes that can match those receiving monthly treatment (Bressler, 2009).

4. Intravitreal injection methodology

4.1. Needle bore

The effect of needle bore size may be investigated using Poiseuille's law which defines the flow of material in a tube system (Chuang et al., 2008) in relation to the radius of the tube. Furthermore, the needle bore size may have a secondary effect on the post-injection IOP which influences the pharmacokinetics of the IVT as discussed later. Significantly higher IOP spikes were noted with intravitreal injections using smaller needle bore sizes (Kim et al., 2008a).

4.2. Choice of scleral injection site and reflux

The location of the intravitreal injection was found to have a substantial effect on material distribution and elimination in the vitreous (Friedrich et al., 1997). In that study, a mathematical model that had been developed and used previously to study drug distribution in the vitreous humour of the rabbit eye was modified to match the physiology of the human eye. Fluorescein and fluorescein glucuronide were used as the model compounds. Four injection locations were considered which mapped the extremes of possibilities: a central injection, an injection displaced towards the retina, an injection displaced towards the lens, and an injection displaced towards the hyaloid membrane. Peak concentrations at different vitreous locations were found to vary by over three orders of magnitude, depending on the injection location. The mean concentration of drug remaining in the vitreous 24 h after the intravitreal injection varied by up to a factor of 3.8, depending on the injection location. Increasing the volume of the injection from 15 μL to 100 μL dampened the effects of the initial injection location; however, mean concentrations at 24 hours still varied by up to a factor of 2.5.

A significant fraction of injections with bevacizumab (46%) was found to be associated with reflux of clear fluid after the removal of the needle (Boon et al., 2008) although the fluid was not thought to contain significant amount of the drug itself. They also found that most of the patients who were noted to have reflux were likely to show similar amount of reflux with subsequent injections, suggesting that certain characteristics of the eye could influence this.

The amount of fluid reflux following intravitreal injection of bevacizumab could be reduced by modification of the injection technique using a tunneled scleral incision by Rodrigues et al. (2007). In another study, the amount of pegaptanib reflux was also reduced by modification of the injection technique by introducing the needle at an oblique angle to the scleral site (Lopez-Guajardo et al., 2008). In both studies, the amount of reflux was assessed objectively by measuring the subconjunctival bleb dimensions using ultrasound biomicroscopy.

4.3. The effects of intraocular pressure changes

When injecting anti-VEGF agent, a consequent rise in intraocular pressure (IOP) is considered to be self-limiting (Benz et al., 2006). However, this phenomenon needs to be considered from a drug distribution perspective since an increase in IOP can generate a steeper pressure gradient between the anterior chamber and the retinal surface, which in turn results in faster convective flow and enhanced drug deposition to the retina. This has been simulated by finite element modelling (Park et al., 2005) and the temporary rise in intraocular pressure could potentially reduce the half-life of anti-VEGF agents (Xu et al., 2000). Short-term IOP changes have been widely reported after ranibizumab and bevacizumab injections in humans (Kim et al., 2008a). Recently, researchers have demonstrated sustained rises of IOP for more than one month after injection of anti-VEGF medications in AMD patients with no pre-existing risk factors, such as a personal or family history of glaucoma or ocular hypertension (Adelman, 2009). Cases of severe and sustained ocular hypertension have also been reported by Bakri et al. (2008) after intravitreal ranibizumab and have been attributed to the way different compounding pharmacies prepare doses of ranibizumab. This may lead to differences in high molecular weight adducts that may plug outflow pathways or cause an immunologic response in the trabecular meshwork that leads to IOP spikes (Bakri et al., 2008).

The role of VEGF as a neuroprotectant has raised several concerns over the potential neurotoxic effects of anti-VEGF agents. The combination of anti-VEGF and IVT-associated IOP spikes could potentially result in progressive retinal ganglion cell (RGC) loss and retinal nerve fibre layer thinning in susceptible patients. However, there is to date no evidence from short or long term studies in humans to support this and the emerging studies on rodents and cell cultures are reassuring, since they have failed to demonstrate RGC toxicity even after repeated intravitreal injections (Cheng et al., 2009; Iriyama et al., 2007; Kim et al., 2008b). A minority of animal studies have shown bevacizumab to exert a moderate growth inhibition on choroidal endothelial cells and RPE cells (Spitzer et al., 2006), as well as rabbit photoreceptor cells (Avci et al., 2009). Further studies would be required to determine how the elderly human eye behaves when there is co-existing age-related RGC loss or pre-existing ocular pathology, such as normal tension glaucoma

Please cite this article in press as: Laude, A., et al., Intravitreal therapy for neovascular age-related macular degeneration and..., Progress in Retinal and Eye Research (2010), doi:10.1016/j.preteyeres.2010.04.003

or open angle glaucoma, in order to establish the risk of visual loss arising from progressive RGC loss.

Whilst prophylaxis to prevent IOP spikes is not current clinical practice, it may be considered for patients who show an IOP rise that is considered clinically significant after IVT. Studies on acquired immunodeficiency syndrome (AIDS) and AMD patients have demonstrated the value of ocular massage or use of Honan balloon for this purpose (Jager et al., 2004), and there have been reports of a few cases of severe and sustained ocular hypertension after intravitreal ranibizumab that required control with topical glaucoma therapy and in two cases the addition of a systemic carbonic anhydrase inhibitor (Bakri et al., 2008).

The risks of anterior chamber paracentesis and potential anterior chamber shallowing, forward lens displacement and altered vitreous drug distribution make this intervention necessary only if central retinal artery obstruction occurs. Predicting which individuals experiencing this complication and visual loss arising from progressive retinal ganglion cell loss and retinal nerve fibre layer thinning from IVT-associated IOP spikes requires further investigation. Interestingly, corneal thickness and scleral rigidity are known to influence IOP measurements but are also etiologically linked to AMD risk. Recent reports suggesting anti-VEGF induced retinal ganglion cell apoptosis may also be relevant to risk assessment of IVT in AMD.

5. Conclusion and future directions

Despite previous experiences of IVT in other clinical contexts, for example the intravitreal injections of antivirals in viral retinitis associated with AIDS or antibiotics for bacterial endophthalmitis, the relative expense, prolonged duration and safety concerns in an elderly target population mandate a closer evaluation of a tailored approach to individualized IVT in AMD. Further studies are needed to drive improvements in clinical practice aimed at maximizing the efficacy profile in IVT for AMD by a more rigorous evaluation of patient and surgeon-related variables.

Based on clinical experience and published reports from models to randomized controlled trials (RCTs), further studies to define association between ocular anatomy and outcomes are recommended. This might be achieved by expanding the relevance of perfused eye models in parallel with more rigorous examination of ocular biometric variables on therapeutic responses. These data may then be incorporated into an IVT care model together with routinely collected outcomes on psychophysics and quality of life as a move towards individual patient-focused AMD care.

Acknowledgment

We are grateful to Adelekan Oyejide, Allergan for his contributions in the examinations of the histological cross-sections of animal ocular tissues (Fig. 1).

Financial support

AL is supported by Tan Tock Seng Scholarship and LET is the recipient of an open educational grant from Allergan Inc.

Statement

The authors do not have any proprietary interest in any inventions or scientific matter discussed in this paper.

References

Adelman, R., 2009. Persistent ocular hypertension associated with intravitreal anti-VEGF. In: American Academy of Ophthalmology Joint Annual Meeting San Francisco, USA.

Aguilar, H.E., Meredith, T.A., el-Massry, A., Shaarawy, A., Kincaid, M., Dick, J., Ritchie, D.J., Reichley, R.M., Neisman, M.K., 1995. Vancomycin levels after intravitreal injection. Effects of inflammation and surgery. Retina 15, 428–432.

Avci, B., Avci, R., Inan, U.U., Kaderli, B., 2009. Comparative evaluation of apoptotic activity in photoreceptor cells after intravitreal injection of bevacizumab and pegaptanib sodium in rabbits. Invest. Ophthalmol. Vis. Sci. 50, 3438–3446.

Bakri, S.J., McCannel, C.A., Edwards, A.O., Moshfeghi, D.M., 2008. Persistent ocular hypertension following intravitreal ranibizumab. Graefes Arch. Clin. Exp. Ophthalmol. 246, 955–958.

Bakri, S.J., Snyder, M.R., Reid, J.M., Pulido, J.S., Singh, R.J., 2007. Pharmacokinetics of intravitreal bevacizumab (Avastin). Ophthalmology 114, 855–859.

Barza, M., Kane, A., Baum, J., 1982. The effects of infection and probenecid on the transport of carbenicillin from the rabbit vitreous humor. Invest. Ophthalmol. Vis. Sci. 22, 720–726.

Barza, M., Kane, A., Baum, J., 1983. Pharmacokinetics of intravitreal carbenicillin, cefazolin, and gentamicin in rhesus monkeys. Invest. Ophthalmol. Vis. Sci. 24, 1602–1606.

Benz, M.S., Albini, T.A., Holz, E.R., Lakhanpal, R.R., Westfall, A.C., Iyer, M.N., Carvounis, P.E., 2006. Short-term course of intraocular pressure after intravitreal injection of triamcinolone acetonide. Ophthalmology 113, 1174–1178.

Boon, C.J., Crama, N., Klevering, B.J., van Kuijk, F.J., Hoyng, C.B., 2008. Reflux after intravitreal injection of bevacizumab. Ophthalmology 115, 1270. author reply 1271.

Bressler, N.M., 2009. Antiangiogenic approaches to age-related macular degeneration today. Ophthalmology 116, S15–23.

Cheng, C.K., Peng, P.H., Tien, L.T., Cai, Y.J., Chen, C.F., Lee, Y.J., 2009. Bevacizumab is not toxic to retinal ganglion cells after repeated intravitreal injection. Retina 29, 306–312.

Chin, H.S., Park, T.S., Moon, Y.S., Oh, J.H., 2005. Difference in clearance of intravitreal triamcinolone acetonide between vitrectomized and nonvitrectomized eyes. Retina 25, 556–560.

Chuang, G.S., Rogers, G.S., Zeltser, R., 2008. Poiseuille's law and large-bore needles: insights into the delivery of corticosteroid injections in the treatment of keloids. J. Am. Acad. Dermatol. 59, 167–168.

Cobo, L.M., Forster, R.K., 1981. The clearance of intravitreal gentamicin. Am. J. Ophthalmol. 92, 59–62.

Dadgostar, H., Ventura, A.A., Chung, J.Y., Sharma, S., Kaiser, P.K., 2009. Evaluation of injection frequency and visual acuity outcomes for ranibizumab monotherapy in exudative age-related macular degeneration. Ophthalmology 116, 1740–1747.

Drolet, D.W., Nelson, J., Tucker, C.E., Zack, P.M., Nixon, K., Bolin, R., Judkins, M.B., Farmer, J.A., Wolf, J.L., Gill, S.C., Bendele, R.A., 2000. Pharmacokinetics and safety of an anti-vascular endothelial growth factor aptamer (NX1838) following injection into the vitreous humor of rhesus monkeys. Pharm. Res. 17, 1503–1510.

Eter, N., 2008. Ranibizumab for Neovascular ARMD: Results of the EXCITE and SUSTAIN Studies. German Retina Society, Wurzburg, Germany.

Falavarjani, K.G., Modarres, M., Nazari, H., 2010. Therapeutic effect of bevacizumab injected into the silicone oil in eyes with neovascular glaucoma after vitrectomy for advanced diabetic retinopathy. Eye 24, 717–719.

Ficker, L., Meredith, T.A., Gardner, S., Wilson, L.A., 1990. Cefazolin levels after intravitreal injection. Effects of inflammation and surgery. Invest. Ophthalmol. Vis. Sci. 31, 502–505.

Fishman, G.A., Cunha-Vaz, J., Salzano, T., 1981. Vitreous fluorophotometry in patients with retinitis pigmentosa. Arch. Ophthalmol. 99, 1202–1207.

Foulds, W.S., Allan, D., Moseley, H., Kyle, P.M., 1985. Effect of intravitreal hyaluronidase on the clearance of tritiated water from the vitreous to the choroid. Br. J. Ophthalmol. 69, 529–532.

Foy, J.W., Rittenhouse, K., Modi, M., Patel, M., 2007. Local tolerance and systemic safety of pegaptanib sodium in the dog and rabbit. J. Ocul. Pharmacol. Ther. 23, 452–466.

Friedrich, S., Cheng, Y.L., Saville, B., 1997. Drug distribution in the vitreous humor of the human eye: the effects of intravitreal injection position and volume. Curr. Eye Res. 16, 663–669.

Fung, A.E., Rosenfeld, P.J., Reichel, E., 2006. The international intravitreal bevacizumab safety survey: using the internet to assess drug safety worldwide. Br. J. Ophthalmol. 90, 1344–1349.

Gan, I.M., Ugahary, L.C., van Dissel, J.T., van Meurs, J.C., 2005. Effect of intravitreal dexamethasone on vitreous vancomycin concentrations in patients with suspected postoperative bacterial endophthalmitis. Graefes Arch. Clin. Exp. Ophthalmol. 243, 1186–1189.

Gaudreault, J., Fei, D., Rusit, J., Suboc, P., Shiu, V., 2005. Preclinical pharmacokinetics of ranibizumab (rhuFabV2) after a single intravitreal administration. Invest. Ophthalmol. Vis. Sci. 46, 726–733.

Gisladottir, S., Loftsson, T., Stefansson, E., 2009. Diffusion characteristics of vitreous humour and saline solution follow the Stokes Einstein equation. Graefes Arch. Clin. Exp. Ophthalmol. 247, 1677–1684.

Heegaard, S., Jensen, O.A., Prause, J.U., 1986. Structure and composition of the inner limiting membrane of the retina. SEM on frozen resin-cracked and enzyme-digested retinas of Macaca mulatta. Graefes Arch. Clin. Exp. Ophthalmol. 224, 355–360.

Please cite this article in press as: Laude, A., et al., Intravitreal therapy for neovascular age-related macular degeneration and..., Progress in Retinal and Eye Research (2010), doi:10.1016/j.preteyeres.2010.04.003

Heiduschka, P., Fietz, H., Hofmeister, S., Schultheiss, S., Mack, A.F., Peters, S., Ziemssen, F., Niggemann, B., Julien, S., Bartz-Schmidt, K.U., Schraermeyer, U., 2007. Penetration of bevacizumab through the retina after intravitreal injection in the monkey. Invest. Ophthalmol. Vis. Sci. 48, 2814–2823.

Hughes, P.M., 2008. Topical delivery to the retina: reality or artifact. In: Angiogenesis, Exudation and Degeneration Meeting. Bascom Palmer Eye Institute, Florida.

Hughes, P.M., Olejnik, O., Chang-Lin, J.E., Wilson, C.G., 2005. Topical and systemic drug delivery to the posterior segments. Adv. Drug Deliv. Rev. 57, 2010–2032.

Iriyama, A., Chen, Y.N., Tamaki, Y., Yanagi, Y., 2007. Effect of anti-VEGF antibody on retinal ganglion cells in rats. Br. J. Ophthalmol. 91, 1230–1233.

Jaffe, N.S., 1969. The Vitreous in Clinical Ophthalmology. The C.V. Mosby Company, USA.

Jager, R.D., Aiello, L.P., Patel, S.C., Cunningham Jr., E.T., 2004. Risks of intravitreous injection: a comprehensive review. Retina 24, 676–698.

Jongebloed, W.L., Worst, J.F., 1987. The cisternal anatomy of the vitreous body. Doc. Ophthalmol. 67, 183–196.

Kim, J.E., Mantravadi, A.V., Hur, E.Y., Covert, D.J., 2008a. Short-term intraocular pressure changes immediately after intravitreal injections of anti-vascular endothelial growth factor agents. Am. J. Ophthalmol. 146, 930–934. e931.

Kim, J.H., Kim, C., Lee, B.J., Yu, Y.S., Park, K.H., Kim, K.W., 2008b. Absence of intravitreal bevacizumab-induced neuronal toxicity in the retina. Neurotoxicology 29, 1131–1135.

Knudsen, L.L., Dissing, T., Hansen, M.N., Nielsen-Kudsk, F., 2001. Ocular fluorescein kinetics before and after vitrectomy on swine. Graefes Arch. Clin. Exp. Ophthalmol. 239, 832–839.

Koeberle, M.J., Hughes, P.M., Skellern, G.G., Wilson, C.G., 2006. Pharmacokinetics and disposition of memantine in the arterially perfused bovine eye. Pharm. Res. 23, 2781–2798.

Lee, S.S., Ghosn, C., Yu, Z., Zacharias, L.C., Kao, H., Lanni, C., Abdelfattah, N., Kuppermann, B., Csaky, K.G., D'Argenio, D.Z., Burke, J.A., Hughes, P.M., Robinson, M.R., 2010. Vitreous VEGF clearance is increased following vitrectomy. Invest. Ophthalmol. Vis. Sci. 51, 2135–2138.

LMNO Engineering and Software, Ltd. http://www.lmnoeng.com/Volume/CylConeSphere.htm#References.

Lopez-Cortes, L.F., Pastor-Ramos, M.T., Ruiz-Valderas, R., Cordero, E., Uceda-Montanes, A., Claro-Cala, C.M., Lucero-Munoz, M.J., 2001. Intravitreal pharmacokinetics and retinal concentrations of ganciclovir and foscarnet after intravitreal administration in rabbits. Invest. Ophthalmol. Vis. Sci. 42, 1024–1028.

Lopez-Guajardo, L., Del Valle, F.G., Moreno, J.P., Teus, M.A., 2008. Reduction of pegaptanib loss during intravitreal delivery using an oblique injection technique. Eye 22, 430–433.

Lund-Andersen, H., Sander, B., 2003. The vitreous. In: Kaufman, P.L., Alm, A. (Eds.), Adler's Physiology of the Eye, tenth. Mosby Inc, USA, pp. 293–316.

Lunt, R., 1978. Handbook of Ultrasonic B-Scanning in Medicine. Cambridge University Press Archive, Cambridge, pp. 18.

Majumdar, S., Kansara, V., Mitra, A.K., 2006. Vitreal pharmacokinetics of dipeptide monoester prodrugs of ganciclovir. J. Ocul. Pharmacol. Ther. 22, 231–241.

Mandell, B.A., Meredith, T.A., Aguilar, E., el-Massry, A., Sawant, A., Gardner, S., 1993. Effects of inflammation and surgery on amikacin levels in the vitreous cavity. Am. J. Ophthalmol. 115, 770–774.

Mannermaa, E., Vellonen, K.S., Urtti, A., 2006. Drug transport in corneal epithelium and blood-retina barrier: emerging role of transporters in ocular pharmacokinetics. Adv. Drug. Deliv. Rev. 58, 1136–1163.

Maurice, D.M., 1976. Injection of drugs into the vitreous body. In: Leopold, I., Burns, R (Eds.), Symposium on Ocular Therapy. John Wiley & Sons, Inc., New York, pp. 59–72.

Maurice, D., 2001. Review: practical issues in intravitreal drug delivery. J. Ocul. Pharmacol. Ther. 17, 393–401.

Maurice, D.M., Mishima, S., 1984. Ocular pharmacokinetics. In: Sears, M.L. (Ed.), Handbook of Experimental Pharmacology: Pharmacology of the Eye. Springer-Verlag, Berlin, pp. 19–116.

Meredith, T.A., 2006. Intravitreal antimicrobials. In: Jaffe, G.J., Ashton, P., Pearson, P. A. (Eds.). Intraocular Drug Delivery, Taylor and Francis, UK, pp. 85–93.

Meredith, T.A., Aguilar, H.E., Shaarawy, A., Kincaid, M., Dick, J., Niesman, M.R., 1995. Vancomycin levels in the vitreous cavity after intravenous administration. Am. J. Ophthalmol. 119, 774–778.

Missel, P.J., 2002. Hydraulic flow and vascular clearance influences on intravitreal drug delivery. Pharm. Res. 19, 1636–1647.

Mitchell, P., Korobelnik, J.F., Lanzetta, P., Holz, F.G., Pruente, C., Schmidt-Erfurth, U.M., Tano, Y., Wolf, S., 2010. Ranibizumab (Lucentis) in neovascular age-related macular degeneration: evidence from clinical trials. Br. J. Ophthalmol. 94, 2–13.

Moldow, B., Larsen, M., Sander, B., Lund-Andersen, H., 2001. Passive permeability and outward active transport of fluorescein across the blood-retinal barrier in early ARM. Br. J. Ophthalmol. 85, 592–597.

Moldow, B., Sander, B., Larsen, M., Engler, C., Li, B., Rosenberg, T., Lund-Andersen, H., 1998. The effect of acetazolamide on passive and active transport of fluorescein across the blood-retina barrier in retinitis pigmentosa complicated by macular oedema. Graefes Arch. Clin. Exp. Ophthalmol. 236, 881–889.

Moldow, B., Sander, B., Larsen, M., Lund-Andersen, H., 1999. Effects of acetazolamide on passive and active transport of fluorescein across the normal BRB. Invest. Ophthalmol. Vis. Sci. 40, 1770–1775.

Moseley, H., Foulds, W.S., Allan, D., Kyle, P.M., 1984. Routes of clearance of radioactive water from the rabbit vitreous. Br. J. Ophthalmol. 68, 145–151.

Ogura, Y., Tsukada, T., Negi, A., Honda, Y., 1989. Integrity of the blood-ocular barrier after intravitreal gas injection. Retina 9, 199–202.

Oguro, Y., Tsukahara, Y., Saito, I., Kondo, T., 1985. Estimation of the permeability of the blood-retinal barrier in normal individuals. Invest. Ophthalmol. Vis. Sci. 26, 969–976.

Park, J., Bungay, P.M., Lutz, R.J., Augsburger, J.J., Millard, R.W., Sinha Roy, A., Banerjee, R.K., 2005. Evaluation of coupled convective–diffusive transport of drugs administered by intravitreal injection and controlled release implant. J. Control Release 105, 279–295.

Peeters, L., Sanders, N.N., Braeckmans, K., Boussery, K., Van de Voorde, J., De Smedt, S.C., Demeester, J., 2005. Vitreous: a barrier to nonviral ocular gene therapy. Invest. Ophthalmol. Vis. Sci. 46, 3553–3561.

Pflugfelder, S.C., Hernandez, E., Fliesler, S.J., Alvarez, J., Pflugfelder, M.E., Forster, R.K., 1987. Intravitreal vancomycin. Retinal toxicity, clearance, and interaction with gentamicin. Arch. Ophthalmol. 105, 831–837.

Pitkanen, L., Pelkonen, J., Ruponen, M., Ronkko, S., Urtti, A., 2004. Neural retina limits the nonviral gene transfer to retinal pigment epithelium in an in vitro bovine eye model. AAPS J. 6, e25.

Prager, T.C., Chu, H.H., Garcia, C.A., Anderson, R.E., 1982. The influence of vitreous change on vitreous fluorophotometry. Arch. Ophthalmol. 100, 594–596.

Richtig, E., Langmann, G., Mullner, K., Richtig, G., Smolle, J., 2004. Calculated tumour volume as a prognostic parameter for survival in choroidal melanomas. Eye 18, 619–623.

Rodrigues, E.B., Meyer, C.H., Grumann Jr., A., Shiroma, H., Aguni, J.S., Farah, M.E., 2007. Tunneled scleral incision to prevent vitreal reflux after intravitreal injection. Am. J. Ophthalmol. 143, 1035–1037.

Rosenfeld, P.J., Schwartz, S.D., Blumenkranz, M.S., Miller, J.W., Haller, J.A., Reimann, J. D., Greene, W.L., Shams, N., 2005. Maximum tolerated dose of a humanized anti-vascular endothelial growth factor antibody fragment for treating neovascular age-related macular degeneration. Ophthalmology 112, 1048–1053.

Sander, B., Larsen, M., Moldow, B., Lund-Andersen, H., 2001. Diabetic macular edema: passive and active transport of fluorescein through the blood-retina barrier. Invest. Ophthalmol. Vis. Sci. 42, 433–438.

Schindler, R.H., Chandler, D., Thresher, R., Machemer, R., 1982. The clearance of intravitreal triamcinolone acetonide. Am. J. Ophthalmol. 93, 415–417.

Short, B.G., 2008. Safety evaluation of ocular drug delivery formulations: techniques and practical considerations. Toxicol. Pathol. 36, 49–62.

Singh, S., Stewart, J.M., 2008. Intraocular bevacizumab for iris neovascularization in a silicone oil-filled eye. Retin. Cases Brief. Rep 2, 253–255.

Spitzer, M.S., Wallenfels-Thilo, B., Sierra, A., Yoeruek, E., Peters, S., Henke-Fahle, S., Bartz-Schmidt, K.U., Szurman, P., 2006. Antiproliferative and cytotoxic properties of bevacizumab on different ocular cells. Br. J. Ophthalmol. 90, 1316–1321.

Stay, M.S., Xu, J., Randolph, T.W., Barocas, V.H., 2003. Computer simulation of convective and diffusive transport of controlled-release drugs in the vitreous humor. Pharm. Res. 20, 96–102.

Tan, L.E., 2009. Effects of vitreous liquefaction on the intravitreal distribution of sodium fluorescein, fluorescein dextran and fluorescent microparticles. In: ARVO Summer Eye Research Conference, NIH, Bethseda, USA.

Wu, L., Martinez-Castellanos, M.A., Quiroz-Mercado, H., Arevalo, J.F., Berrocal, M.H., Farah, M.E., Maia, M., Roca, J.A., Rodriguez, F.J., 2008. Twelve-month safety of intravitreal injections of bevacizumab (Avastin): results of the Pan-American Collaborative Retina Study Group (PACORES). Graefes Arch. Clin. Exp. Ophthalmol. 246, 81–87.

Xu, J., Heys, J.J., Barocas, V.H., Randolph, T.W., 2000. Permeability and diffusion in vitreous humor: implications for drug delivery. Pharm. Res. 17, 664–669.

Yoshida, A., Furukawa, H., Delori, F.C., Bursell, S.E., Trempe, C.L., McMeel, J.W., 1984. Effect of vitreous detachment on vitreous fluorophotometry. Arch. Ophthalmol. 102, 857–860.

Zhu, Q., Ziemssen, F., Henke-Fahle, S., Tatar, O., Szurman, P., Aisenbrey, S., Schneiderhan-Marra, N., Xu, X., Grisanti, S., 2008. Vitreous levels of bevacizumab and vascular endothelial growth factor-A in patients with choroidal neovascularization. Ophthalmology 115, 1750–1755.

Please cite this article in press as: Laude, A., et al., Intravitreal therapy for neovascular age-related macular degeneration and..., Progress in Retinal and Eye Research (2010), doi:10.1016/j.preteyeres.2010.04.003